Superoxide Produced in the Heme Pocket of the β-Chain of Hemoglobin Reacts with the β-93 Cysteine To Produce a Thiyl Radical[†]

Chavali Balagopalakrishna,[‡] Omoefe O. Abugo,[‡] Jiri Horsky,[‡] Periakaruppan T. Manoharan,[§] Enika Nagababu,[‡] and Joseph M. Rifkind*,[‡]

Gerontology Research Center, National Institute on Aging, National Institutes of Health, 5600 Nathan Shock Drive, Baltimore, Maryland 21224-6823, and Department of Chemistry, Regional Sophisticated Instrumentation Center, Indian Institute of Technology, Madras 600-036, India

Received April 27, 1998; Revised Manuscript Received July 27, 1998

ABSTRACT: The role of the β-93 cysteine residue in the hemoglobin autoxidation process has been delineated by electron paramagnetic resonance. At low temperatures (8 K) after incubation at 235 K, free radical signals were detected. An analysis of the free radical spectrum produced implies that, besides the superoxide radical expected to be formed during autoxidation, an isotropic free radical is produced with a g_{iso} of 2.0133. This g value is consistent with that expected for a sulfur radical. Blocking the β-93 sulfhydryl group with *N*-ethylmaleimide was found to eliminate the formation of the isotropic radical, but not the superoxide. This finding confirms the assignment of the isotropic radical as a thiyl radical originating from the oxidation of the cysteine SH group. A kinetic analysis of the time course for the formation of both the superoxide and thiyl radicals is consistent with a reversible electron transfer process between superoxide in the heme pocket of the β-chains and the cysteine residue. This reaction is expected to produce both a thiyl radical and a peroxide. Direct evidence for peroxide production comes from the detection of a transient Fe(III) heme peroxide complex. The significance of the electron transfer process producing a thiyl radical is discussed. It is shown that the formation of the thiyl radical decreases the rate of autoxidation for the β-chain and reduces heme degradation attributed to the reaction of superoxide with the heme. The insights gained from these low-temperature studies are believed to be relevant to room-temperature autoxidation.

During reversible oxygen binding, hemoglobin undergoes a slow autoxidation to physiologically inactive ferric hemoglobin, producing superoxide. The autoxidation process is clinically and chemically important, and its mechanism has been extensively studied (*1*−*5*), although many details are still unresolved.

Studies show that increased heme pocket fluctuations (*6*) for partially oxygenated hemoglobin under hypoxic conditions facilitate the displacement of bound oxygen as a superoxide, resulting in enhanced rates of autoxidation (*3*, *7*−*9*). At 235 K, the superoxide radical formed is trapped in the hydrophobic heme pocket. This superoxide was detected and identified by low-temperature electron paramagnetic resonance spectroscopy (EPR)[1] (*10*). Spontaneous dismutation, which requires two superoxide molecules, can occur only after the superoxide leaves the heme pocket, a process which is very slow at 235 K.

In this paper, we have investigated a possible reaction occurring with this reactive superoxide radical formed at the ligand binding site of hemoglobin prior to leaving the heme pocket. Evidence for the formation of a thiyl radical indicates an electron transfer reaction involving an SH group and the superoxide in the heme pocket. The occurrence of this reaction is also supported by detection of a ferric heme peroxide complex. The β-93 cysteine residue, the only sulfhydryl-containing group in close proximity, is known to influence the oxygen affinity and oxidation of the heme iron and its physicochemical properties (*11*−*17*). This study delineates the role of the cysteine residue in the autoxidation process.

EXPERIMENTAL PROCEDURES

Preparation of Hemoglobin Samples. The red blood cells obtained from healthy participants of the Baltimore Longitudinal Study on Aging were hemolysed by freeze-thawing after washing three times with phosphate-buffered saline (PBS, pH 7.4) to remove the buffy coat and plasma. The lysed cells were subjected to centrifugation at 18 000 rpm for 30 min to remove the membranes. Although these samples contain superoxide dismutase and catalase, which can influence autoxidation, they are not expected to alter the reactions studied in this paper at 235 K.

Partial deoxygenation of the hemoglobin samples was carried out in a Labconco controlled environment glovebox. Two different concentrations (0.07 and 7.38 mM) of hemoglobin were deoxygenated to specified partial pressures

[†] P.T.M. was supported by USIF Project N-426-645 as well as by a position from the Council of Scientific and Industrial Research, India.

* Corresponding author: Molecular Dynamics Section, Laboratory of Cellular & Molecular Biology, Gerontology Research Center, National Institute on Aging, 5600 Nathan Shock Dr., Baltimore, MD 21224-6823. Telephone: (410) 558-8168. Fax: (410) 558-8173.

[‡] National Institutes of Health.

[§] Indian Institute of Technology.

[1] Abbreviations: EPR, electron paramagnetic resonance; NEM, *N*-ethylmaleimide; Hb, hemoglobin.

S0006-2960(98)00941-6
Published on Web 08/29/1998

of O_2 and equilibrated by gentle rocking. At each pO_2, aliquots from the more concentrated samples were transferred to 4 mm outside diameter quartz EPR tubes, which were quickly frozen in liquid nitrogen inside the glovebox. Aliquots from the dilute samples were transferred to cells with ground glass joints for measurements in a visible spectrophotometer (Perkin-Elmer Lambda 6) to determine the concentrations of oxyhemoglobin, deoxyhemoglobin, and methemoglobin and to measure the rate of autoxidation.

Thiol (β-93)-blocked hemoglobin samples were prepared (*17*) from hemolysed cells. A 10-fold excess of *N*-ethylmaleimide (NEM) was added to the hemolysed cells and the mixture allowed to react for 2 h. This procedure (*17*) results in the reaction of NEM exclusively with the β-93 cysteine residue. The NEM-reacted hemoglobin (NEM−Hb) was then dialyzed against 0.1 M NaCl overnight followed by dialysis against PBS to remove the unreacted NEM. The resulting sample was respun to remove residual ghosts and precipitated material. More than 98% of the reactive sulfhydryl groups were blocked in the clear NEM−Hb prepared in this way. The NEM−Hb was then used for the preparation of partially oxygenated samples in the manner described above for the untreated hemoglobin.

Electron Paramagnetic Resonance Measurements. Electron paramagnetic resonance (EPR) spectra were measured at 7−8 K using an IBM ER-200D-SRC spectrometer with 100 kHz modulation and an Air Products model LTD-3-110 liquid transfer Heli-tran cryogenic unit with an APD-E temperature controller. The microwave frequency was calibrated using an EIP model 548A microwave frequency counter. Incubation of EPR samples was carried out in a Cryotrol Cryobath (CB-80, Neslab Instruments Inc.) maintained at 235 K.

Fluorescence Measurements. Fluorescence measurements were taken using a Perkin-Elmer 650-40 fluorescence spectrophotometer at 295 K. Normal hemoglobin and NEM−Hb reacted with hydrogen peroxide under normoxic conditions that were used to study (*18*) the formation of the heme degradation fluorescent product with an excitation wavelength of 321 nm and an emission wavelength of 465 nm.

EPR Simulation. The experimental spectra were simulated with "EPR−A MODELING APPROACH", written in Pascal (*19*). The spin Hamiltonian used is

$$\hat{H} = \beta\vec{\mathbf{B}}\mathbf{g}\hat{S} + S\mathbf{D}\hat{S} + \sum_{i=1}^{10}\hat{F}_i\mathbf{A}^{(\mathbf{I})}S \qquad (1)$$

The three terms represent the electron−zeeman, electron−electron dipolar, and nuclear hyperfine interactions, respectively. $\hat{F}$ is the nuclear spin angular momentum operator summed over those of the *i*th subgroup of equivalent nuclei; i.e., $\hat{F} = \sum_{i=1}^{n} I_i$. The coordinates are referenced to the diagonal components of the **g** tensor. This program can fit an experimental spectrum to multiple components by adding the individual spectral components according to

$$S(H) = \sum f_i \bar{S}_i(H) \qquad (2)$$

where $S(H)$ is the total EPR spectrum of the sample and $\bar{S}_i(H)$ is the constituent spectrum from its *i*th species weighted by the factor f_i.

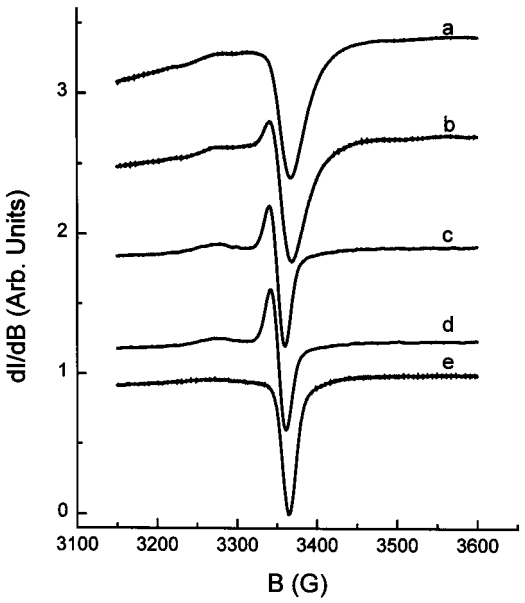

FIGURE 1: X-Band EPR spectra of partially oxygenated hemoglobin (55.8% oxyhemoglobin, 38.2% deoxyhemoglobin, and 6% methemoglobin) at 8 K after different 235 K incubation times: (a) 0 min, (b) 3 min, (c) 7 min, and (d) 17 min and (e) a fully thawed sample. Only the $g_{||}$ region of methemoglobin from 3200 to 3500 G is shown.

Our experimental spectra were simulated with either two species (methemoglobin and the superoxide radical) or three species (methemoglobin, superoxide, and an isotropic radical). Simulations were performed by varying f_i of eq 2, the **g** tensors, and the line width tensors (ω), while maintaining the same values for θ and φ (*19*). Default values were used for all other parameters. A typical simulation took about 5 min of computer time on a 486 personal computer.

Analysis of Kinetic Data. The kinetic data were analyzed with the use of MLAB, a mathematical modeling program by Civilized Software, Inc. (Bethesda, MD). This program makes it possible to fit complex kinetic models by either analytical or numerical solutions.

RESULTS

Electron Paramagnetic Resonance Studies on Nonmodified Hemoglobin. The EPR spectra of partially oxygenated hemoglobin (containing 55.8% oxyhemoglobin, 38.2% deoxyhemoglobin, and 6% methemoglobin) were recorded after incubation for different periods of times at 235 K (Figure 1). The figure clearly shows the time-dependent changes that appear in the region (from 3200 to 3500 G) of the $g_{||}$ component of methemoglobin. Within the first 3 min, line shape changes due to the growth of new signals were observed. These new features found in Figure 1 completely disappear on thawing the samples at 298 K (Figure 1e), leaving behind only the $g_{||}$ signal due to methemoglobin.

The nature of these new features is shown in Figure 2 by subtracting the underlying $g_{||}$ of methemoglobin from spectrum d in Figure 1. This subtraction was accomplished by using the integrated intensity of the methemoglobin high-spin $g_{\perp}$ at low field (900−1300 G) to subtract off the underlying $g_{||}$ part of this spectrum. The resultant spectrum has a $g_{||}$ of 2.0563 and a $g_{\perp}$ of 2.0043, which are consistent with the reported (*20*, *21*) spectrum of superoxide. A careful examination of the shape of the new $g_{\perp}$ signal, however,

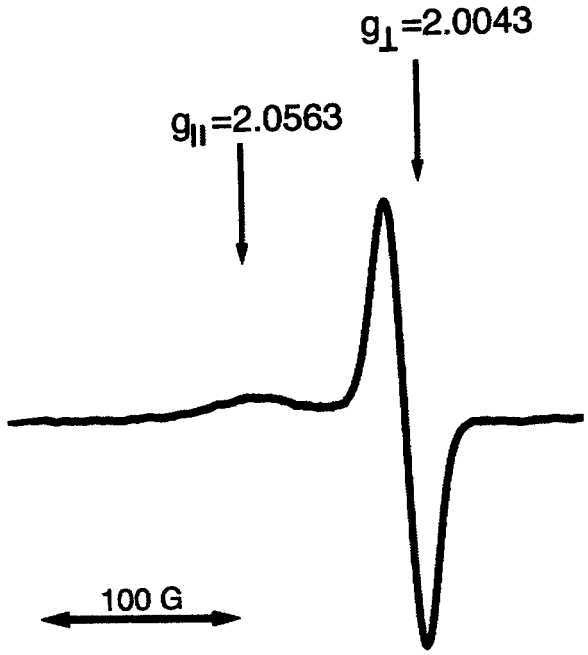

FIGURE 2: X-Band EPR spectrum of partially oxygenated hemoglobin of spectrum d of Figure 1 after subtraction of its metHb content (see the text).

indicates a line shape different from that expected for the $g_\perp$ component usually associated with the axially symmetric superoxide signal (*20*, *21*). The observed spectrum is much more isotropic than that reported for superoxide.

This discrepancy suggests the presence of an extra signal in addition to the resonant absorptions from methemoglobin and superoxide. This premise is further confirmed by the poor fit (Figure 3) obtained for spectrum d of Figure 1 with a two-species model composed of only methemoglobin and the superoxide radical. The discrepancy is easily discerned from the inability to fit the highly positive slope of the first derivative line. This positive slope produces more of an isotropic line shape to the anisotropic $g_\perp$ signal.

A much improved fit to the experimental spectrum was obtained by assuming a three-species model with the inclusion of a third isotropic radical at $g_{iso} = 2.0133$ as shown in the right panel of Figure 3. By varying the concentrations of methemoglobin, superoxide, and the third isotropic radical, we could fit all the experimental spectra of Figure 1 as shown in Figure 4. These results establish the time dependence for the formation of a second radical species during the hypoxic autoxidation of hemoglobin.

Electron Paramagnetic Resonance on NEM-Modified Hemoglobin. The high *g* value associated with the third species ($g_{iso} = 2.0133$) points to the involvement of a heavy atom such as sulfur (*22*) and the suggestion that a thiyl radical is being formed during the heme autoxidation process. To confirm this possibility, the β-93 cysteine sulfhydryl group, the only reactive SH group on hemoglobin, was blocked by NEM (*17*). The NEM−Hb was then partially deoxygenated under conditions similar to those used for the untreated hemoglobin samples. Because of the higher oxygen affinity of NEM−Hb (*23*), it was necessary to equilibrate with a lower partial pressure of oxygen to obtain a similar level of oxygenation. The sample produced had 48% oxyhemoglobin, 39% deoxyhemoglobin, and 13% methemoglobin. EPR measurements were performed under the same incubation conditions used for untreated hemoglobin. The resulting EPR spectra are shown in Figure 5. The superoxide signal growth over the methemoglobin $g_{||}$ signal looks similar to that of the NEM-untreated hemoglobin sample (Figure 1). However, the $g_\perp$ feature in these spectra is less isotropic, and they could be fit with a two-species model containing only superoxide and methemoglobin (Figure 6). This analysis clearly demonstrates that the second radical produced during autoxidation under hypoxia must originate from the β-93 cysteine group and is probably a thiyl radical.

Formation of a Heme Peroxy Complex. The reaction of superoxide with an SH group to produce a thiyl radical would produce a peroxide in the heme pocket. Low-spin Fe(III) peroxy complexes (*24*) display rhombic EPR spectra and frequently have a g_3 of slightly less than 2. To determine whether such a signal is formed, it was necessary to improve the resolution in this region of the spectrum. This improved resolution was accomplished by subtracting off the $g_{||}$ signal of methemoglobin from the spectrum by the same method used to obtain Figure 2. The spectrum shown in Figure 7 reveals the presence of a resonant absorption at $g = 1.94$, supporting the hypothesis that the additional radical is associated with the reduction of the superoxide to a peroxide.

Kinetic Modeling. The time-dependent changes in the relative concentration of the superoxide radical and the other protein radical, viz. the thiyl radical (vide infra), are shown in Figure 8. The relative concentrations of the free radicals were obtained from their corresponding EPR intensities. For this purpose, a justifiable assumption was made that both radical species have the same electron relaxation time at the low temperature of measurement. An estimate of the concentration of the free radicals relative to that of the hemoglobin would require double integration of the entire methemoglobin signal in the initial preincubation hemoglobin sample which contains 6% methemoglobin. The total hemoglobin intensity would be 16.7 times that intensity, while the initial oxyhemoglobin intensity involved in the autoxidation would be 9.3 times the methemoglobin intensity. This intensity must then be compared with double integration of the relatively sharp free radical signals. A quantitative determination of these relative concentrations is very difficult because of the large uncertainty in the integration of methemoglobin signals which extend over more than 3000 G. In addition, the electron relaxation times for methemoglobin and the free radicals are not expected to be the same. It is, however, evident by comparison of the signal intensities that the concentration of the free radicals (both superoxide and thiyl radicals) are not more than a few percent of the oxyhemoglobin.

To quantify the relationship between the formation of these two radical species and the autoxidation process, a kinetic model has been used to simulate the autoxidation. As indicated by our EPR studies, it has been assumed that the second radical is a thiyl radical formed by the reaction of superoxide with the β-93 cysteine residue. This assumption requires that the dissociation of the bound oxygen as a superoxide be followed by the formation of a thiyl radical only in the β-chain. In the α-chain, without the cysteine residue, this additional reaction does not take place.

The data in Figure 8 indicate that the concentration of the superoxide radical peaks out at about 10 min (incubation at

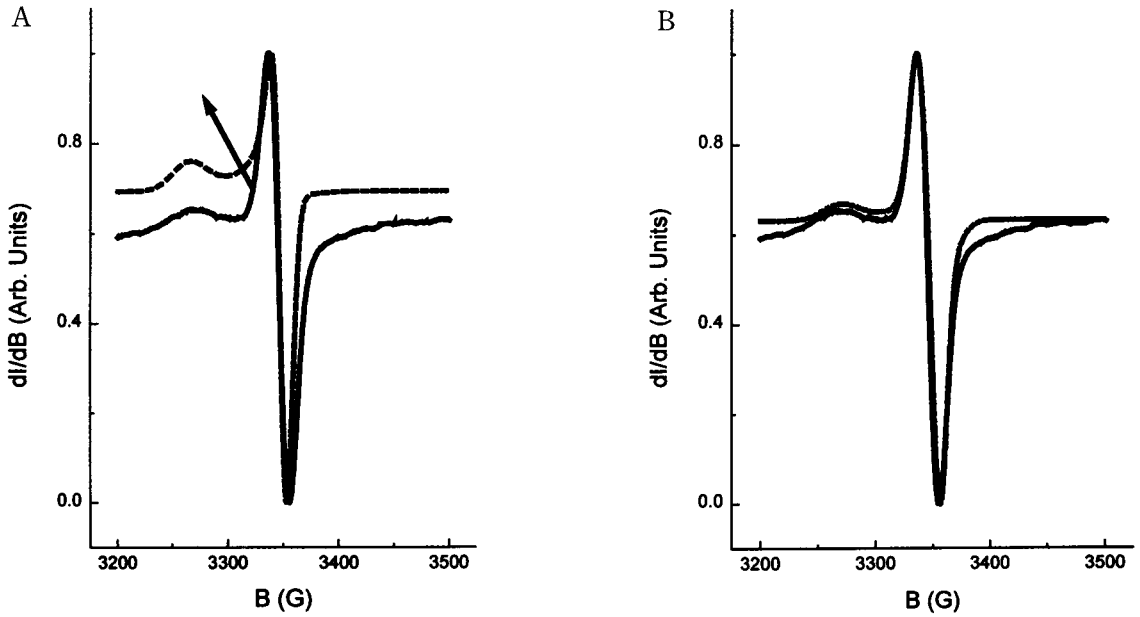

FIGURE 3: Simulation of EPR spectrum after incubation for 17 min. (A) Comparison of the experimental EPR spectrum d of Figure 1 (—) and its simulation (···) with a two-component model with only the $g_{||}$ part of metHb (g = 2.0023, ω = 14.6 G) and the anisotropic superoxide radical ($g_x = g_y$ = 2.0067, g_z = 2.0593, $\omega_x = \omega_y$ = 7.5 G, ω_z = 18 G). (B) Comparison of the experimental EPR spectrum shown in spectrum d of Figure 1 (—) and the simulated spectrum (···) using a three-component model containing the $g_{||}$ part of metHb (g = 2.0023, ω = 14.6 G), the anisotropic superoxide radical ($g_x = g_y$ = 2.0067, g_z = 2.0593, $\omega_x = \omega_y$ = 7.5 G, ω_z = 18 G), and an isotropic radical with a g_{iso} of 2.0133 and a ω_{iso} of 9.5 G.

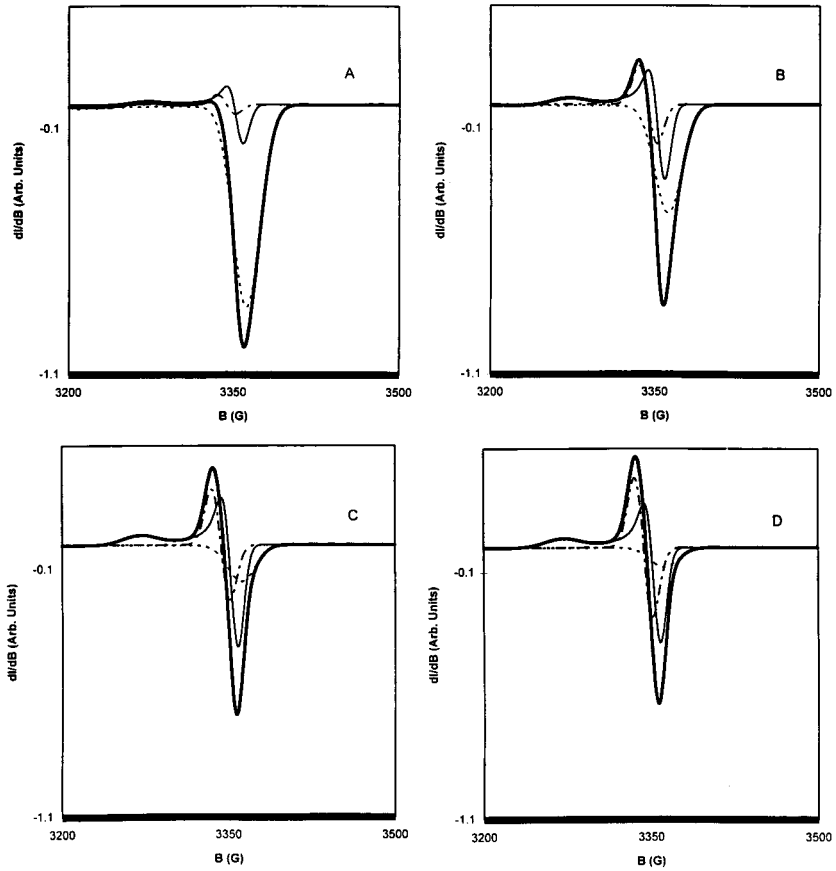

FIGURE 4: Simulation of spectra a−d of Figure 1 using a three-component model: experimental (−), $g_{||}$ and $g_{\perp}$ of superoxide (−), $g_{||}$ of metHb (···), and isotropic free radical (−·−) with the same parameters used in Figure 3.

235 K) and then begins to decrease, while the rate of formation of the thiyl radical increases for about 15 min and then seems to level off. The relatively low radical concentrations (see above) at these times are inconsistent with all of the oxyhemoglobin being converted to superoxide. To explain the low concentrations of the radicals, it is necessary to postulate that oxyhemoglobin exists in multiple substates (*25*) which interconvert very slowly at the low temperature

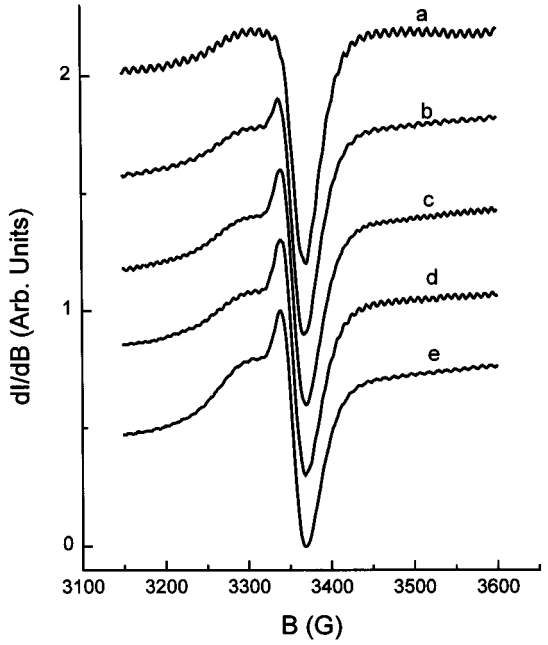

FIGURE 5: X-Band EPR spectra of partially oxygenated NEM-blocked hemoglobin (48% oxyhemoglobin, 39% deoxyhemoglobin, and 13% methemoglobin) at 8 K for different incubation times at 235 K: (a) 0, (b) 3, (c) 7, (d) 17, and (e) 37 min. The spectral region is the same as that in Figure 1.

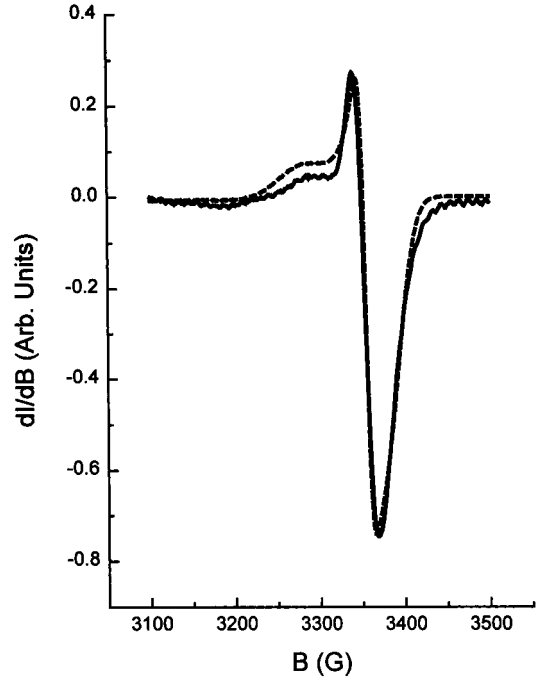

FIGURE 6: X-Band EPR spectrum d of Figure 5 (—) and its simulation (•••) using a two-component model (superoxide and metHb) with the same parameters used in Figure 3.

(*6*, *26*) used in our experiments. Presumably, only a small fraction of these substates participate in the low-temperature autoxidation reaction.

When the formations of both radical species are compared in Figure 8, it is found that superoxide is produced more rapidly than the thiyl radical. This is consistent with the model which proposes that the superoxide is produced by autoxidation while the thiyl radical is only produced by the subsequent secondary reaction of the superoxide with the cysteine residue. The finding that the relative concentration

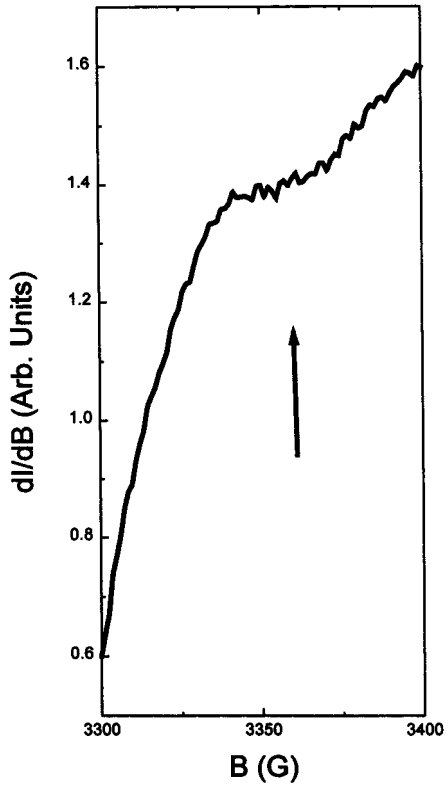

FIGURE 7: X-Band EPR spectral feature on the high-field shoulder of spectrum b of Figure 1 after subtracting off the metHb signal using the $g_{\perp}$ at 6.0.

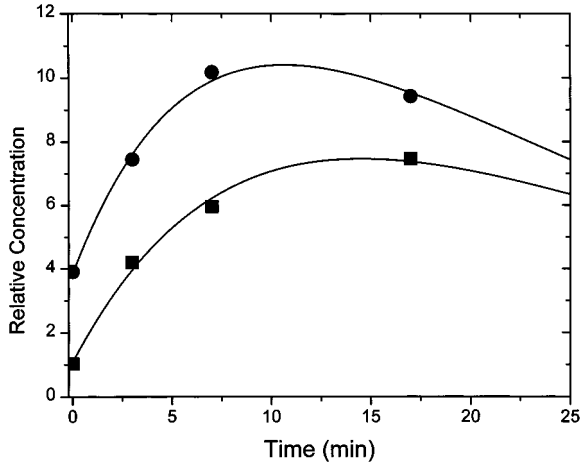

FIGURE 8: Relative concentration of superoxide (●) and thiyl radical (■) as a function of incubation time at 235 K in partially oxygenated Hb obtained from EPR simulations shown in Figure 4. The lines correspond to a fit to the kinetic model as indicated in the text.

of superoxide actually increases while the thiyl radical is forming, with appreciable concentrations of superoxide still present at the longest time points, is partly explained by the superoxide formed in the α-chain. To properly fit the experimental data, it was, however, necessary to postulate that (1) superoxide formed in the heme pocket disappears during the course of the reaction and (2) the reaction of the superoxide to produce the thiyl radical is reversible. The disappearance of the superoxide could be attributed to slow reactions with the heme or globin, which do not give EPR-resolved signals, and/or a slow leakage out of the globin where it can dismutate.

The model used to fit the data (Figure 8) is shown below:

$$\mathrm{Ox}_\alpha \xrightarrow{k_1} \mathrm{S}_\alpha + \mathrm{Fe}^+ \quad (\downarrow k_3)$$

$$\mathrm{Ox}_\beta \xrightarrow{k_2} \mathrm{S}_\beta + \mathrm{Fe}^+ \underset{k_5}{\overset{k_4}{\rightleftharpoons}} \mathrm{T} + \mathrm{Pr} \quad (\downarrow k_3)$$

where Ox is the oxygenated substate involved in autoxidation, S is the superoxide contained in the heme pocket, Fe^+ is the oxidized heme iron, T is the thiyl radical, and Pr is the peroxide. It has been assumed that at the low temperatures used in our experiments (235 K) all of the reactions are taking place within the heme pocket and, therefore, follow first-order kinetics. We have furthermore assumed that the rate for the disappearance of superoxide (k_3) was the same for both chains. The rate constant values which gave the best least-squares fit to the data (Figure 8) are as follows: $k_1 = 0.073$ min^{-1}, $k_2 = 0.067$ min^{-1}, $k_3 = 0.141$ min^{-1}, $k_4 = 226$ min^{-1}, and $k_5 = 186$ min^{-1}. This model considers different values for the reaction of Ox_α and Ox_β (i.e., k_1 and k_2) in forming superoxide. Although it is not expected that these rate constants should be the same for α- and β-chains, the two rate constants obtained in the fit are quite similar. The large values of k_4 and k_5 indicate that the superoxide reacts very rapidly with the cysteine. However, we found that the fit was relatively insensitive to the actual values for k_4 and k_5 as long as the ratio of k_4/k_5 remained equal to 1.22.

This model considers differences between the α- and β-chains with respect to the displacement of oxygen as a superoxide (k_1 and k_2), but not in the rate for the disappearance of superoxide (k_3). The data do not justify adding an additional constant to the model. However, the alternative model with k_1 equal to k_2 and the value of k_3 being different for α- and β-chains was considered. In this alternative model, $k_1 = 0.07$ min^{-1} which is equal to the average rate for the formation of superoxide in the initial model. There was appreciable variation in the rates for the disappearance of superoxide with a $k_{3\alpha}$ of 0.156 min^{-1} and a $k_{3\beta}$ of 0.132 min^{-1}, resulting in an average value of 0.144 min^{-1}, almost identical to the value of k_3 in the initial model. This model produces a decrease in the equilibrium constant for the formation of the thiyl radical from 1.22 to 1.14. This decrease is expected so the same level of thiyl radical can be maintained under conditions where the superoxide radical disappears from the heme pocket more slowly. Because of a slightly better fit for the initial model than this alternative model, we have used the initial model with only one value of k_3 in the rest of the discussion.

Fluorescence. Figure 9 shows the time-dependent production of the 465 nm fluorescence (321 nm excitation) for the reaction of the unreacted hemoglobin and NEM−Hb with hydrogen peroxide. It has been shown that hemoglobin oxidized by hydrogen peroxide produces two fluorescent compounds (*18*) which have been attributed to heme degradation products formed by the reaction of superoxide in the ligand pocket with the heme (*18*). The significant increase in this heme degradation product for NEM−Hb indicates that the free sulfhydryl plays a role in protecting the heme from superoxide damage.

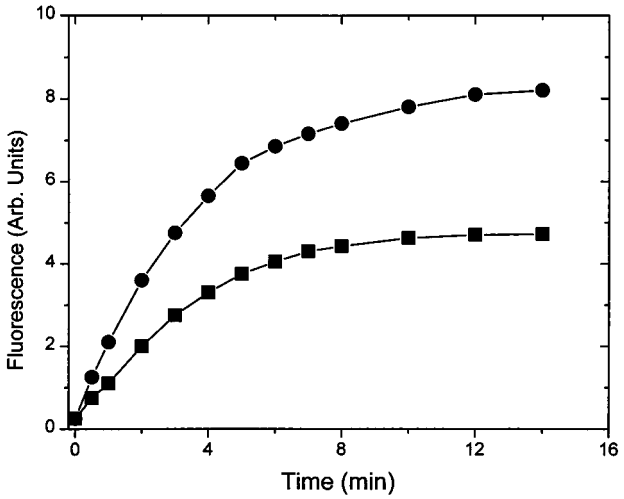

FIGURE 9: Time course of fluorescence intensity for the emission at 460 nm obtained at an excitation wavelength of 321 nm for normal hemoglobin (■) and NEM−Hb (●).

DISCUSSION

Reaction of Superoxide To Produce a Second Radical. During the autoxidation process, oxygen is displaced from oxyhemoglobin as a superoxide radical, which is released into the heme pocket (*9*, *10*). We have, in fact, shown that under hypoxic conditions with an elevated concentration of partially oxygenated hemoglobin intermediates, autoxidation is appreciably more rapid (*3*, *27*). Under these conditions, the superoxide trapped in the heme pocket was directly detected by low-temperature EPR (*10*). At 235 K, the trapped superoxide was, as shown in Figures 1 and 5, stable for extended periods of time. The extended lifetime of superoxide in the hydrophobic heme pocket can partially be explained by the inability of an isolated superoxide to spontaneously dismutate. Furthermore, superoxide is much less reactive than many other free radicals and does not indiscriminately react with everything with which it comes in contact. Instead, its relatively long lifetime facilitates reaction at even relatively remote sites sensitive to either oxidation or reduction by superoxide (*28*).

By comparing the free radical signal generated during 235 K autoxidation with that reported for superoxide (Figure 2), we have in this paper demonstrated that there is a reaction of the superoxide in the heme pocket with the globin producing a secondary radical. Thus, the subtraction of the $g_{||}$ component of methemoglobin from spectrum d of Figure 1 yields an isotropic free radical signal (Figure 2) which lacks the expected anisotropy of the superoxide radical (*20*, *21*). Furthermore, the spectra in Figure 1 cannot be fit with a two-component model containing only methemoglobin and the superoxide radical (Figure 3), but require a third component. The nearly perfect fit observed in Figure 4 with three components establishes the presence of a new protein-derived free radical.

It is also possible to show that this second radical is a consequence of autoxidation of hemoglobin and is not due to any impurity. Thus, this species was not present prior to incubation, and it was not present on thawing the hypoxic sample to room temperature, which results in the disappear-

ance of all the free radical signals. Moreover, incubation of pure deoxy- or methemoglobin, which do not have oxygen bound to the heme, under identical conditions does not produce either of the free radical signals (*10*).

The analysis of the relative intensities of the $g_{||}$ of methemoglobin, $g_{||}$ and $g_{\perp}$ of superoxide, and an isotropic radical with a g_{iso} of 2.0133 at the different incubation times shown in Figure 4 provides convincing evidence for the formation of both radical species during the autoxidation process. The time-dependent changes in the relative concentrations of these two radical species are shown (Figure 8) to be consistent with a reaction of the superoxide with the globin, at least in one of the globin chains, to produce a secondary radical. The formation of secondary protein radicals has been shown to take place during the oxidation reactions of hemoglobin involving hydrogen peroxide (*29*) and phenylhydrazine (*30*).

An electron transfer reaction involving the superoxide is confirmed by the detection (Figure 7) of a resonance at $g = 1.94$. Such a signal is observed in other hemoproteins and iron complexes and is generally associated with g_3 of a low-spin Fe(III) heme peroxy complex (*24*), which is produced as a result of the one-electron reduction of superoxide.

Identification of the Secondary Radical. The features of the additional isotropic signal can be used to identify its origin. Since most low-spin complexes have axial or rhombic **g** tensors, the absence of the other components and also the smaller line width of isotropic nature preclude the possibility of it being a low-spin iron complex (*31*, *32*). Furthermore, the lack of hyperfine features rules out nitrogen- or proton-centered radicals, while the high g_{iso} value of 2.0133 rules out carbon- or oxygen-centered radicals. The EPR characteristics are best explained by a free radical with an atomic center which has a large spin−orbit coupling constant such as sulfur. This analysis raises the possibility that the globin-based radical formed during autoxidation could originate from a thiyl radical coming from a cysteine residue. Also, the g_{iso} value conforms with an earlier report of thiyl radicals originating from cysteine-containing systems (*33*).

The β-93 cysteine, with the only chemically reactive sulfhydryl group on hemoglobin (*12*−*17*, *23*), is located ∼14 Å from the iron (*34*) in the proximity of the heme pocket where superoxide is produced. This residue is, therefore, a likely candidate for the production of a thiyl radical. This assignment was confirmed by using NEM to specifically block this reactive sulfhydryl group (*17*). As shown in Figure 5, superoxide radicals are also produced during incubation of NEM−Hb. However, the shapes of the signals in Figure 5 are different from those observed with the free sulfhydryl group in Figure 1 (the signal is more anisotropic). Furthermore, the spectra of NEM-reacted hemoglobin are properly fit with two components involving only methemoglobin and the superoxide radical (Figure 6) without the need for the isotropic signal with a g_{iso} of 2.0133. The thiyl radical detected in the absence of NEM can thus be attributed to a reaction of the superoxide released into the heme pocket with the β-93 sulfhydryl located in the same vicinity (*34*).

Role of the Thiyl Radical in Autoxidation. The EPR studies establish the existence of a second reaction whereby the superoxide formed in the β-chain can react with the β-93 cysteine residue to form a thiyl radical. The modeling of this reaction makes it possible to relate this reaction to the overall autoxidation process. The requirement for a reversible reaction with the sulfhydryl indicates a facile shuttling of electrons between the cysteine reside on the proximal side of the heme and the superoxide in the ligand pocket on the distal side of the heme, even at 235 K.

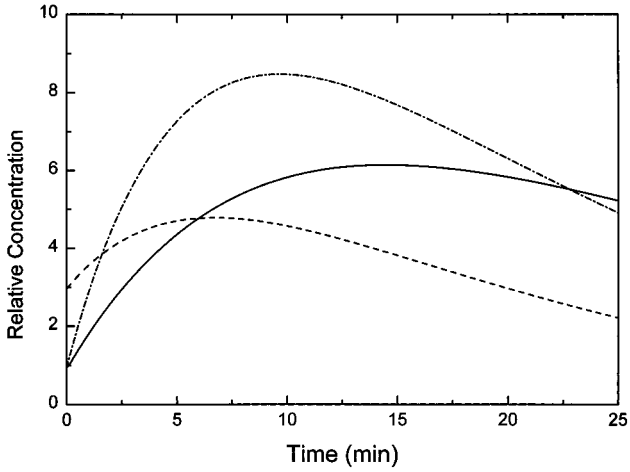

FIGURE 10: Effect of thiyl radical formation on the relative concentration of superoxide in the α-chain (− −) and the β-chain (—) and the effect of setting k_4 and k_5 equal to zero on the superoxide concentration in the β chain (−•−).

The electron transfer reaction proposed to take place between the superoxide and the cysteine residue extends over a number of bonds. However, even longer-range electron transfer reactions have been shown to readily occur in various metalloenzymes (*35*−*38*) . The conformation in the region of the β-93 cysteine residue changes during oxygenation (*39*), affecting the reactivity of the cysteine residue with sulfhydryl reagents (*40*). Nevertheless, since the distances (*34*) between the heme iron and a mercury atom bound to the sulfur of the β-93 cysteine residue are 14.3 and 13.6 Å in the oxy and deoxy conformations of hemoglobin, respectively, the electron transfer process is not expected to be particularly sensitive to conformation. This process should, therefore, influence the autoxidation process irrespective of the hemoglobin conformation.

It is also necessary to consider a possible effect of blocking the sulfhydryl group on the displacement of the bound oxygen as a superoxide (the k_1, k_2 process) which would, thereby, influence the autoxidation. Blocking the sulfhydryl group stabilizes the liganded *R* conformation of hemoglobin (*39*), and its effect on the autoxidation should be dependent on this quaternary conformational change. This effect is, however, not relevant to our experiments which were performed at similar levels of oxygenation. The NEM sample was at 55% oxygenation actually slightly less oxygenated then the non-NEM sample at 59% oxygenation, compensating for any shift in the quaternary conformation because of NEM.

The modeling is not very sensitive to the actual rate for this electron transfer reaction, although it does establish the ratio of the rate constants k_4/k_5 or the equilibrium constant for the formation of the thiyl radical. As indicated in Figure 10, the superoxide concentration in the heme pocket during the early stages of the reaction is much lower in the β-chain, which undergoes the reaction forming a thiyl radical, than in the α-chain, where this reaction does not take place. Also

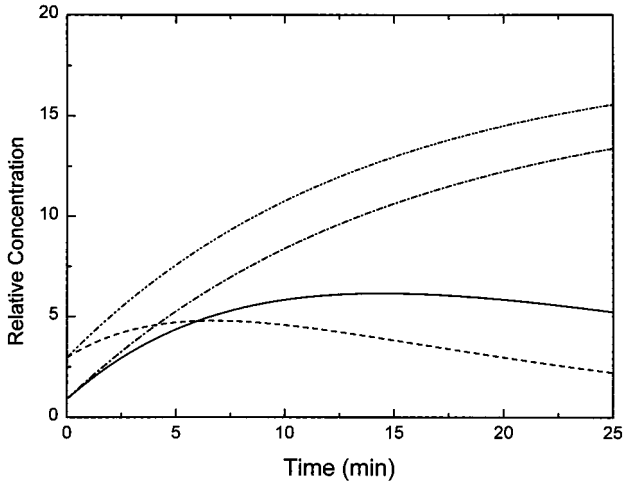

FIGURE 11: Effect of thiyl radical formation on the relative concentration of superoxide in the α-chain (− −) and the β-chain (—) and the effect of setting k_3 equal to zero on the α-chain (−••−) and β-chain (−•−).

shown in Figure 10 is the very significant increase in the level of β-chain superoxide when blocking the β-93 sulfhydryl is modeled by setting k_4 and k_5 equal to zero. These results suggest that thiyl radical formation is responsible for decreasing superoxide production. A similar trend was observed for the alternative model with different rate constants for the k_3 process in the α- and β-chains.

As long as the electron involved in autoxidation is associated with the thiyl radical, it can be reshuffled back to the heme iron via the superoxide. Therefore, the rate-limiting step for autoxidation is the disappearance of the superoxide from the heme pocket, k_3. The flux of superoxide in the heme pocket can be determined by comparing the superoxide levels measured with those obtained when k_3 is set equal to zero. As shown in Figure 11, this flux is much smaller for the β-chain than the α-chain, which supports our hypothesis that the fast electron transfer involving thiyl radicals protects the heme from autoxidation.

These studies were performed at low temperatures. The relationship between these low-temperature studies and autoxidation at room temperature has been established by the correlation between rates of autoxidation at room temperature and the levels of free radicals produced at low temperatures for samples with different levels of oxygenation (*10*). It has also been shown (*41*) that the free radical intermediates produce oxidation. Thus, the signal intensities of the methemoglobin bands increase when the sample is thawed and refrozen after the 235 K incubation, which produces the free radical intermediates.

The studies on the effect of the thiyl radical on autoxidation can, therefore, be used to predict relative rates of autoxidation in α- and β-chains and the effect of blocking the sulfhydryl. At elevated temperatures, the electron transfer process between the superoxide and the β-93 cysteine residue will be even faster. Therefore, the lower steady state for superoxide found the β-chain as well as the lower rate of autoxidation for the β-chain found at low temperatures should be retained at elevated temperatures. This prediction explains the finding that in fresh hemolysates more of the α-chains are oxidized than the β-chains (*42*). These results are also consistent with results in the literature which implicate the sulfhydryl in oxidation and reduction processes involving hemoglobin (*14*, *15*, *43*, *44*). It is also expected that the rate of autoxidation should increase if the β-93 sulfhydryl is blocked. However, since the free sulfhydryl also dramatically increases the rate of copper-induced oxidation (*43*, *45*, *46*), this enhanced rate of autoxidation will only be detected if trace levels of copper are removed. This requirement explains previous reports (*14*) that *N*-ethylmaleimide decreases the rate of oxidation.

Disappearance of Superoxide, a Possibility of Heme Degradation. The reaction associated with the disappearance of the superoxide (k_3) can be attributed to leakage of the superoxide out of the heme pocket. However, because of the reactivity of the superoxide, it is also necessary to consider possible reactions of the superoxide with the heme and/or globin. The potential for such secondary reactions is enhanced because of the restricted motion in the globin at 235 K which appreciably increases the time required for ligands to go into or out of the heme pocket (*6*, *25*, *26*) and, thereby, the lifetime of superoxide in the heme pocket.

Such a secondary interaction involving the reaction of superoxide with the heme is supported by studies on superoxide-induced heme degradation. We have, thus, shown (*18*) that superoxide produced in the heme pocket as a result of the reaction of ferryl hemoglobin with hydrogen peroxide causes heme degradation even at room temperature. This degradation process was quantified by the measurement of fluorescent heme degradation products. The relationship between this heme degradation process and the stability of the superoxide in the heme pocket is indicated by the effect of blocking the β-93 cysteine residue (Figure 9). Thus, the production of one of these fluorescent products (excitation at 321 nm and emission at 465 nm) is shown to increase about 80% (Figure 9) during the reaction with hydrogen peroxide, when the sulfhydryl is blocked by NEM. As seen in Figure 10, the reaction of the sulfhydryl with the superoxide to produce a thiyl radical lowers the level of superoxide in the heme pocket. This decrease in the level of superoxide would presumably be responsible for the decrease in the level of heme degradation (Figure 9). These heme degradation products may eventually accumulate into membranes causing membrane damage.

Hemoglobin Substates Involved in Autoxidation. The analysis of the time dependence for the superoxide and thiyl radicals (Figure 8) requires that only a small fraction of the oxygenated chains be involved in formation of the radicals at 235 K. As noted above, this observation requires that only certain substates of oxygenated chains be involved in superoxide release. Furthermore, at 235 K, the re-equilibration between these substates is slow. In our earlier analysis of the oxygen dependence of autoxidation and superoxide formation (*3*, *27*), it was concluded that superoxide formation is associated with enhanced distal pocket flexibility (*6*), which facilitates an interaction of the distal histidine with the bound oxygen resulting in the nucleophilic displacement of the oxygen as a superoxide. The authors of previous EPR and Mossbauer studies on methemoglobin and deoxyhemoglobin (*6*, *26*) have investigated substates where the distal histidine is close to the heme iron. It is these substates which are expected to be responsible for the autoxidation. They were shown to be present at low concentrations at room temperature and to be populated only slowly at 235 K. The

current finding regarding a substate responsible for autoxidation is, therefore, consistent with these earlier studies.

Relationship between Hypoxic Thiyl Radical Production and the Release of NO. The relationship between thiyl radical formation and autoxidation has been discussed above. Perhaps even more important than any role in autoxidation is the relationship between thiyl radical formation and hemoglobin S-nitrosylation (*40*, *47*). It has been shown that in vivo a small fraction of the β-93 cysteine residues are nitrosylated (*47*). It has been postulated that low oxygen pressure, i.e., deoxygenation of hemoglobin, facilitates the release of NO from the nitrosylated hemoglobin, causing an increase in capillary blood flow. Although a decreased level of nitrosylation is found in the venous circulation, the mechanism for the release of NO from nitrosylated hemoglobin at low oxygen pressures has not been established.

A linkage between the thiyl radical formation reported in this paper and the release of NO from nitrosylated hemoglobin provides just such a mechanism. It is well-established (*3*, *4*, *10*, *27*) that autoxidation of hemoglobin as well as the release of superoxide into the heme pocket is enhanced at low oxygen pressures, which result in elevated concentrations of partially oxygenated hemoglobin. The formation of the thiyl radical indicates a facile electron exchange between the superoxide and the β-93 cysteine residue. Under conditions where the sulfhydryl is free, this results in a transfer of an electron from the sulfhydryl to the superoxide producing a thiyl radical and a peroxide. Superoxide is known to function both as an oxidizing agent and as a reducing agent (*48*). The release of a superoxide into the β-chain ligand pocket when the cysteine is nitrosylated can, therefore, result in the reduction of the nitrosylated group, coinciding with the release of NO and the oxidation of superoxide back to oxygen. This reaction may thus provide a functional advantage to the enhanced autoxidation at low oxygen pressures, providing a mechanism for the maintenance of blood flow in the microcirculation required for proper oxygen delivery.

REFERENCES

1. Antonini, E., Wyman, J., Brunori, M., Taylor, J. F., Rossi-Fanelli, A., and Caputo, A. (1964) *J. Biol. Chem. 239*, 907−912.
2. Shikama, K. (1984) *Biochem. J. 223*, 279−280.
3. Abugo, O. O., and Rifkind, J. M. (1994) *J. Biol. Chem. 269*, 24845−24853.
4. Wallace, W. J., Houtchens, R. A., Maxwell, J. C., and Caughey, W. S. (1982) *J. Biol. Chem. 257*, 4966−4977.
5. Brantley, R. E., Jr., Smerdon, S. J., Wilkinson, A. J., Singleton, E. W., and Olson, J. S. (1993) *J. Biol. Chem. 268*, 6995−7010.
6. Levy, A., and Rifkind, J. M. (1985) *Biochemistry 24*, 6050−6054.
7. Brooks, J. (1935). *Proc. R. Soc. London, Ser. B 118*, 560−577.
8. George, P., and Stratmann, C. J. (1952) *Biochem. J. 51*, 418−425.
9. Rifkind, J. M., Zhang, L., Heim, J., and Levy, A. (1989) *Oxygen Radicals in Biology and Medicine*, pp 157−166, Plenum Press, New York.
10. Balagopalakrishna, C., Manoharan, P. T., Abugo, O. O., and Rifkind, J. M. (1996) *Biochemistry 35*, 6393−6398.
11. Jocelyn, P. C. (1972) *Biochemistry of the SH Group*, Academic Press, London.
12. Guidotti, G. (1967) *J. Biol. Chem. 242*, 3673−3684.
13. Chiancone, E., Currell, D. L., Vecchini, P., Antonini, E., and Wyman, J. (1970) *J. Biol. Chem. 245*, 4105−4111.
14. Rifkind, J. M. (1972) *Biochim. Biophys. Acta 273*, 30−39.
15. Mansouri, A. (1979) *Biophys. Biochem. Res. Commun. 89*, 441−447.
16. Craescu, C. T., Poyart, C., Schaeffer, C., Garel, M. C., Kister, J., and Beuzard, Y. (1986) *J. Biol. Chem. 261*, 14710−14716.
17. Guidotti, G., and Konigsberg, W. (1964) *J. Biol. Chem. 239*, 1474−1484.
18. Nagababu, E., and Rifkind, J. M. (1998) *Biochem. Biophys. Res. Commun. 247*, 592−596.
19. Neese, F. (1993) Diploma Thesis, University of Konstanz, Konstanz, Germany.
20. Che, M., and Tench, A. J. (1983) *Adv. Catal. 32*, 1−147.
21. Bielski, B. H. J., and Gebicki, J. M. (1982) *J. Am. Chem. Soc. 104*, 796−798.
22. Wertz, J. E., and Bolton, J. R. (1972) *Electron Spin Resonance: Elementary Theory and Practical Applications*, McGraw-Hill, New York.
23. Imai, K. (1973) *Biochemistry 12*, 798−808.
24. Jinno, J., Shigematsu, M., Tajima, K., Sakurai, H., Ohya-Nishiguch, H., and Ishizu, K. (1991) *Biochem. Biophys. Res. Commun. 176*, 675−681.
25. Elber, R., and Karplus, M. (1986) in *Structure, Dynamics and Function of Biomolecules* (Ehrenberg, A., Rigler, R., Gräslund, A., and Nilsson, L., Eds.) pp 15−19, Springer-Verlag, Berlin.
26. Levy, A., Kuppusamy, P., and Rifkind, J. M. (1990) *Biochemistry 29*, 9311−9316.
27. Levy, A., Zhang, L., and Rifkind, J. M. (1988) in *Oxyradicals, Molecular Biology and Pathology* (Cerutti, P. A., Fridovich, I., and McCord, J. M., Eds.) pp 11−25, Alan R. Liss, Inc., New York.
28. Afanas'ev, I. B. (1991) *Superoxide Ion: Chemistry and Biological Implications*, Vol. I, pp 34−58, CRC Press, Boca Raton, FL.
29. Svistunenko, D. A., Patel, R. P., and Wilson, M. T. (1995) *Free Radical Res. 24*, 269−280.
30. Kelman, D. J., and Mason, R. P. (1993) *Arch. Biochem. Biophys. 306*, 439−442.
31. Blumberg, W. E., and Peisach, J. (1971) *Adv. Chem. Ser. 100*, 271−291.
32. Rifkind, J. M., Abugo, O. O., Levy, A., and Heim, J. (1994) *Methods Enzymol. 231*, 449−480.
33. Saxebol, G., and Herskedal, O. (1975) *Radical Res. 62*, 395−406.
34. Muirhead, H., Cox, J. M., Mazzarella, L., and Perutz, M. F. (1967) *J. Mol. Biol. 28*, 117−156.
35. Farver, O., and Pecht, I. (1989) *Proc. Natl. Acad. Sci. U.S.A. 86*, 6968−6972.
36. Geren, L., Hahm, S., Durham, B., and Millett, F. (1991) *Biochemistry 30*, 9450−9457.
37. Stonehuerner, J., O'Brien, P., Geren, L., Millett, F., Steidl, J., Yu, L., and Yu, C. (1985) *J. Biol. Chem. 260*, 5392−5398.
38. Pappa, H. S., and Poulos, T. L. (1995) *Biochemistry 34*, 6573−6580.
39. Perutz, M. F. (1970) *Nature 228*, 726−739.
40. Stamler, J. S., Jia, L., Eu, J. P., McMahon, T. J., Demchenko, I. T., Bonaventura, J., Gernert, K., and Piantadosi, C. A. (1997) *Science 276*, 2034−2037.
41. Levy, A., Abugo, O. O., Franks, M., and Rifkind, J. M. (1991) *J. Inorg. Chem. 43*, 327.
42. Carrell, R. W., Krishnamoorthy, and Winterbourn, C. C. (1978) *Prog. Clin. Biol. Res. 21*, 687−699.
43. Winterbourn, C. C., and Carrell, R. W. (1977) *Biochem. J. 165*, 141−148.
44. Tomoda, A., Yubisui, T., Tsuji, A., and Yoneyama, Y. (1979) *Biochem. J. 197*, 227−231.
45. Rifkind, J. M., Lauer, L. D., Chiang, S. C., and Li, N. C. (1976) *Biochemistry 15*, 5337−5343.
46. Rifkind, J. M. (1979) *Biochemistry 18*, 3860−3865.
47. Jia, L., Bonaventura, C., Bonaventura, J., and Stamler, J. (1996) *Nature 380*, 221−226.
48. Sutton, H. C., Roberts, P. B., and Winterbourn, C. C. (1976) *Biochem. J. 155*, 503−510.

BI980941C